Interface-sensitive conversion-electron Mössbauer study of ion-beam mixing at the Fe-Al interface

V. P. Godbole, S. M. Chaudhari, S. V. Ghaisas, S. M. Kanetkar, and S. B. Ogale
Department of Physics, University of Poona, Pune 411007, Maharashtra, India

V. G. Bhide
School of Energy Studies, University of Poona, Pune 411007, Maharashtra, India
(Received 18 November 1983; revised manuscript received 26 November 1984)

Ion-beam-induced atomic mixing and the effect of thermally activated transformations at the Fe-Al interface have been studied for the first time with use of the technique of conversion-electron ^{57}Fe Mössbauer spectroscopy (CEMS). A concept of interface-sensitive CEMS which exploits the deposition of a thin ($\sim$50-Å) layer of iron enriched to 95.45% of ^{57}Fe at the interface between the aluminium substrate and an overlayer of natural iron (containing only 2.2% of ^{57}Fe) has been introduced and used in the present investigations. CEMS spectra of the as-deposited sample, fitted in terms of the distribution of hyperfine fields at ^{57}Fe nuclei show that not all the ^{57}Fe atoms in the interface region see the environment as in α-Fe but have one or more aluminium neighbors. The interface layers are transformed on bombardment with 100-keV Ar^+ ions at a dose of $\sim 10^{16}$ ions/cm^2 into a random metastable alloy having an average composition of $Fe_{55}Al_{45}$. ^{57}Fe atoms in this alloy experience a variety of environments ranging from dimers in Al matrix at one end to that typically characteristic of α-Fe at the other. This alloy does not show any phase precipitation on vacuum annealing at 300 and 400 °C for 20 min. However, on annealing at 500 °C, a sudden precipitation of α-Fe and Fe_3Al phases is seen. On further annealing of the sample at 600 °C, Fe_3Al phase is seen to decompose to give iron clusters. These results of CEMS measurements have been confirmed by small-angle x-ray-diffraction studies. A non-interface-sensitive CEMS study has also been performed to investigate the dose dependence of ion-beam mixing.

I. INTRODUCTION

In view of the important role played by surfaces in a variety of physical and chemical processes, there is a growing interest particularly in recent years to develop techniques to tailor surface layers on solids to the required specifications. A number of techniques which primarily rely on the concept of directed energy processing of solids have been developed to modify the surface layers. Important and the earliest amongst these is the technique of ion implantation.[1] This process involves forced introduction of desired atoms in solids regardless of the thermodynamic constraints, leading to a possibility of the formation of surface layers with novel properties.[2] Ion implantation has been used in the processing of semiconductor devices and to obtain metastable surface alloys. The method of direct ion implantation has not been highly successful in the formation of surface alloys because of the heavy sputtering associated with high dose implants required for alloy formation. It has been shown recently that this limitation of ion implantation can be eliminated to a considerable extent by using the idea of ion-beam-induced mixing and microalloying of successively deposited thin layers of component materials.[3–11] The high kinetic energy of the incident ions (typically 100—400 keV) produces almost instantly (within a time scale of 10^{-13}—10^{-10} sec) a highly disordered and kinetically active zone across the interface making rapid but transient atomic motions possible. This can lead to alloy formation at an ion dose which is almost 2 orders of magnitude lower than that required in the case of direct ion implantation, thereby eliminating almost entirely, the limitations imposed by sputtering effects. Furthermore, because of the extremely low values of the time scales involved, the alloying induced by ion beam is a highly nonequilibrium process giving rise to metastable alloys. It is generally believed that the reactions that occur during ion-beam mixing are a result of solid-phase interaction of the two materials across the interface, although it is not yet completely clear whether any transient liquid-phase process also contributes to the growth of the metastable phase.[9] Experiments have been carried out to elucidate these points and have provided information on the influence of various parameters such as solid-phase diffusivity,[12] solid solubility,[13] chemical driving force,[14] etc., on the reactions occurring during ion-beam-induced mixing. In all these studies, a variety of techniques, such as, x-ray-diffraction, Rutherford backscattering, and resistivity measurements have been used. Unfortunately, these are all macroscopic techniques and provide little information on atomic motion, environment of atoms of one component in another, etc. Interesting possibility of bringing out information concerning such atomistic details is afforded by Mössbauer spectroscopy, particularly when one of the components involved in ion-beam mixing contains Mössbauer isotopes such as ^{57}Fe, ^{119}Sn, etc. Mössbauer spectroscopy provides a number of windows, such as, isomer shift, quadrupole splitting, magnetic dipole interaction, and the Lamb-Mössbauer factor through which one can obtain valuable information on the nature of chemical environment, magnetic field at nucleus, symmetry of the

neighbors, dynamics of the Mössbauer atoms,[15] etc. This technique can also be made surface-layer sensitive by using conversion-electron Mössbauer spectroscopy (CEMS). In CEMS, the spectra of recoilless resonant γ absorption are registered through the detection of low-energy electrons, such as, 7.3-keV K-shell conversion electrons and 5.4-keV K-LL Auger electrons (in case of ^{57}Fe) and these spectra can thus be made to probe layers as thin as 10—100 nm.[16]

In the present studies we have used the technique of CEMS for the first time to study the physics of ion-beam mixing. In order to selectively probe the ion-beam-induced reactions occurring at the interface we have made our CEMS measurements interface sensitive by enriching the interface layers (thickness $\sim$50 Å) with 95.45% of ^{57}Fe; the overlayer being of natural iron containing only 2.2% of ^{57}Fe. With this contrivance, the Mössbauer spectrum records essentially the signal from ^{57}Fe atoms at the interface. In addition to such interface-sensitive CEMS measurements we have also performed non-interface-sensitive studies wherein the samples were prepared by depositing iron overlayer containing a uniform distribution of ^{57}Fe isotope onto the aluminum substrates. In this case, in order to obtain a good signal-to-noise ratio of the Mössbauer signal the overlayer was uniformly enriched with the ^{57}Fe isotope to 30% in concentration. The reason for carrying out the non-interface-sensitive studies was primarily to reveal the microscopic aspects of the dose dependence of ion-beam mixing. In this context, we resorted to the non-interface-sensitive method due to the fact that the sample preparation for interface-sensitive measurements is conceptually not suitable for the study of dose dependence because it renders a fixed scale of length ($\sim$50 Å) at the interface corresponding to the thickness of ^{57}Fe layer, while the length scale of atomic mixing varies continuously with the ion dose.

In the studies reported in this paper we have attempted to investigate the reactions occurring at the Fe-Al interface due to the process of ion-beam mixing and under subsequent thermal annealing treatment. In addition to the CEMS technique we have also used Rutherford backscattering (RBS) and small-angle x-ray diffraction[17] (Seeman-Bohlin arrangement) techniques to obtain confirmatory support for the information obtained on the basis of CEMS measurements. The reasons for selecting the Fe-Al system are many and obvious. These reasons are (1) ^{57}Fe, a celebrated Mössbauer isotope is a constituent of one of the components involved in the ion-beam-mixing reactions, (2) the normal solubility of Fe in Al is extremely small, i.e., of the order of 0.005 at.% even up to 450 °C,[18] with the result that the conventional equilibrium thermal processing does not yield appreciable intermixing. This system is therefore ideal to bring out the characteristic differences between the ion beam and thermal processing of interfaces, (3) the phase diagram of Fe-Al system has been extensively investigated and shows the existence of a large number of both stable and metastable phases, such as, Fe_4Al_{13}, FeAl, $FeAl_6$, Fe_2Al_5, Fe_3Al, etc. This is a favorable situation in so far as ion-beam mixing is concerned because it has been shown that a system which exists in a large number of phases can be mixed substantially using energetic ion beams.[10] Furthermore, the various phases of this system have been characterized for their x-ray structure and Mössbauer parameters facilitating interpretation of the results obtained in ion-beam-induced reactions. (4) Al being a low Z material produces low photoelectron background in conversion-electron detection, yielding a high signal-to-noise ratio in the CEMS. (5) Al being nonmagnetic, does not create any complications in elucidating magnetic hyperfine interactions at the ^{57}Fe nuclei.

The study reported in this paper has clearly brought out that substantial mixing occurs across the Fe-Al interface leading to a random alloy. In the ion-beam-mixed state this metastable alloy exhibits an interesting magnetic hyperfine interaction pattern and provides evidence for the variety of environments experienced by ^{57}Fe nuclei in this alloy. Thermal annealing of this alloy at and above 500 °C causes atomic motion leading to the precipitation of phases, such as, α-Fe and Fe_3Al. At higher temperatures, Fe_3Al decomposes to form iron clusters. The dose dependence of ion-beam mixing also exhibits interesting features, revealing the microscopic fluctuations of atomic environments.

II. EXPERIMENTAL

Aluminum substrates used in these experiments were cut from ultrapure (99.99% pure) 0.5-mm-thick Al sheet. The cutouts in the form of strips (1 cm$\times$1 cm area) were heat treated in vacuum (10^{-6} Torr) at 600 °C for 8 h to increase the grain size and anneal out the defects and strain. The annealed substrates were cleaned in warm solution of HF, HCl, HNO_3, and double-distilled water in the proportion of 1:10:20:69 to remove contamination and grease on the surface. These substrates were coated with $\sim$50-Å-thick layers of iron enriched to 95.45% in ^{57}Fe concentration by vacuum evaporation. Without breaking the vacuum, this was overcoated with 250-Å-thick layer of natural iron (containing only 2.2% of ^{57}Fe). Since 14.4-keV nuclear γ resonance (Mössbauer effect) emanates from ^{57}Fe, the information obtained through CEMS in the present case is selectively and predominantly from the interface. Care was taken to ensure clean evaporation environment, and the evaporation was carried out at a background pressure of 10^{-6} Torr. The evaporation unit was equipped with foreline traps (molecular sieves) and liquid-nitrogen traps to avoid contamination. For the non-interface-sensitive measurements the samples were prepared by following a similar vacuum evaporation procedure except for the fact that an appropriate quantity of enriched (95.45%) ^{57}Fe was added to natural iron before evaporation, to raise the ^{57}Fe concentration to 30%.

A number of such freshly prepared composites were subjected to Ar^+ ion bombardment (energy 100 keV; dose of $\sim 1\times10^{16}$ ions/cm^2) to induce ion-beam mixing. Ion implantation was carried out using a machine fabricated in our laboratory.[19] The ion current during implantation was maintained in the range of $\sim$1—2 μA/cm^2 so as to avoid appreciable heating of the sample. Ion-beam-induced mixing was confirmed using the Rutherford backscattering technique.

In the interface-sensitive studies, the as-deposited, ion-beam mixed, and subsequently annealed samples were studied using the CEMS technique. For the sake of comparison, the unbombarded composites annealed at various temperatures were also studied. CEMS spectra of the samples were recorded at room temperature using a constant acceleration Mössbauer setup with ^{57}Co:Rh as the source. The 7.3-keV K-shell conversion electrons emitted within 10—100 nm below the top surface were detected in a continuous gas flow (helium + 4% ethanol) proportional counter. To obtain the best-fit values of the hyperfine interaction parameters, computer fitting of the spectra was carried out using the MOSFIT program on ICL 1904S computer.[20] Wherever necessary, the composite Mössbauer spectrum was decomposed into Fourier subspectra following the standard procedure,[21] to provide information on the probability distribution $P(H)$ of the hyperfine field. In the case of the non-interface-sensitive studies, the changes in the spectral features of the CEMS spectra were studied as a function of the ion dose by following similar computer-fitting and Fourier decomposition procedures.

X-ray-diffraction studies on the as-deposited, ion-beam mixed as well as ion-beam mixed and thermally annealed samples were performed by using the small-angle x-ray diffraction technique employing the Seeman-Bohlin arrangement. This technique[17] enables one to obtain structural characterization of a thin (~400—500 Å) layer on a solid surface by enhancing the path traversed by the x rays within the thin layer by almost an order of magnitude.

III. RESULTS AND DISCUSSION

Figure 1 shows the Rutherford backscattering spectra of the as-deposited and ion-beam-mixed samples. The RBS spectrum of the as-deposited sample shows a substrate plateau and the Fe peak. In contrast, the RBS spectrum of the ion-beam-mixed sample shows that atomic mixing has taken place across the interface. It can be deduced that the width of the mixed zone is 100 Å—125 Å across the interface and its average composition is $Fe_{55}Al_{45}$. The RBS measurements clearly show that in spite of an extremely small solubility of iron in aluminum, a concentrated alloy of Fe in Al can be formed by the beam-mixing process, due to its highly nonequilibrium nature.

A. Interface-sensitive CEMS measurements

The conversion-electron Mössbauer spectrum of the as-deposited sample is shown in Fig. 2(a). This spectrum is in many respects similar to the one reported by Preston[22] for ^{57}Fe film deposted on aluminium substrate (Preston used Mössbauer spectroscopy in transmission mode whereas we have used the CEMS mode). The spectrum in Fig. 2(a) can be resolved (as has been done by Preston) into a magnetically split six-line spectrum and a doublet near the zero velocity position; the latter indicative of iron in a nonmagnetic environment. The six-line pattern which corresponds to hyperfine (hf) field of 330 kOe is clearly due to α-Fe, although the linewidths in the present case are much larger than normally expected, indicating the possibility of some distribution in the hf field. In order to gain more insight into the causes of line broadening, we analyzed the Mössbauer spectrum in terms of a continuous distribution of hf field $P(H)$, using a method proposed by Window[21] with the assumption that the sextuplets of probability $P(H)$ have the same average isomer

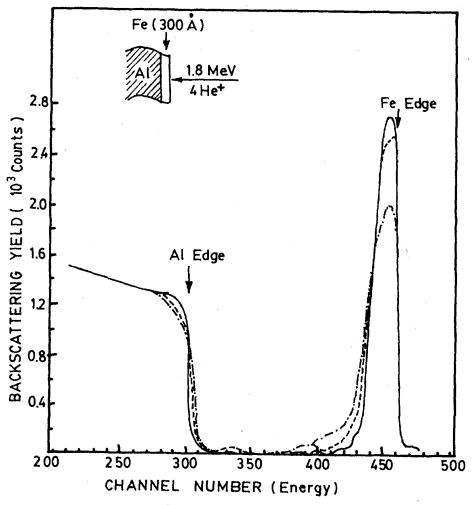

FIG. 1. Rutherford backscattering spectra of the as-deposited and ion-beam-mixed composites. —— corresponds to the as-deposited sample, — — — corresponds to the sample bombarded with 100-keV Ar^+ ions at a dose of 1×10^{16} ions/cm^2, and —·—·—· corresponds to the sample bombarded with 100-keV Ar^+ ions at a dose of 3×10^{16} ions/cm^2.

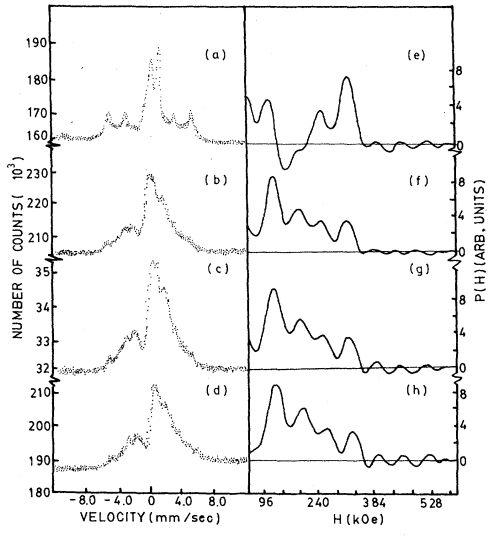

FIG. 2. Room-temperature conversion-electron Mössbauer spectra of (a) as-deposited and (b) ion-beam-mixed Fe-Al composite. The spectra (c) and (d) represent ion-beam-mixed samples annealed at 300 °C and 400 °C, respectively, for 20 min each. The curves in (e), (f), (g), and (h) are the hyperfine field distribution plots corresponding to the spectra in (a), (b), (c), and (d), respectively.

shift and no quadrupole splitting. This $P(H)$ distribution [Fig. 2(e)] shows one peak at ~ 330 kOe characteristic of α-Fe and another at a field value of ~ 252 kOe. Since Al is nonmagnetic, a replacement of an Fe atom by an Al atom in the near neighborhood of ^{57}Fe probe would lead to a reduction in the value of the hf field. It has been estimated that the hf field at ^{57}Fe nucleus reduces linearly at a rate of 26 kOe per Al neighbor.[23] The peak at 252 kOe in the $P(H)$ curve shows unequivocally that some of the ^{57}Fe atoms in the interface region have less than the full complement of iron neighbors as in α-Fe and that some of them have roughly three Al neighbors.

Apart from the two magnetically split spectral components with hf field of ~ 252 kOe and 330 kOe, the Mössbauer spectrum of the as-deposited sample [Fig. 2(a)] shows a central doublet having an isomer shift of 0.33 mm/sec (relative to α-Fe) and a quadrupole splitting of 1.02 mm/sec. Such a doublet may be thought to arise because of three reasons, viz. (i) incorporation of ^{57}Fe in γ-Al_2O_3 skin which is invariably present on the aluminum surface, (ii) presence of α-Fe_2O_3 particles with a particle size less than ~ 100 Å leading to a superparamagnetically relaxed spectrum[24] or (iii) formation of a phase such as $FeAl_6$ which is dilute in Fe concentration and hence yields a nonmagnetic spectrum. We carried out some additional experiments as well as analysis to arrive at a definite conclusion regarding the state of the interface in the as-deposited sample. Firstly, we prepared a sample in which the ^{57}Fe layer was deposited on the aluminum substrate after the deposition of an intermediate spacer layer of ~ 50 Å of natural ion (containing only 2.2% ^{57}Fe). In this case the central doublet contribution became negligibly small, meaning thereby that the proximity of the ^{57}Fe layer to the aluminum substrate is necessary for the occurrence of the doublet. This experiment also helped in eliminating the second possibility of the formation of α-Fe_2O_3 clusters because, if oxidation of the ^{57}Fe layer was the cause of the occurrence of the doublet, the effects of oxidation of iron should have been observed even in the case when the ^{57}Fe layer was away from the aluminum surface. However, neither a superparamagnetic doublet nor a magnetic six-line pattern corresponding to any of the magnetic oxide phases of iron was observed. In order to confirm that the nature of the substrate has a role to play in leading to a central doublet component in the spectrum we prepared additional samples for interface-sensitive studies on other substrates, viz., silicon[25] and germanium.[26] A central doublet was observed in both these cases; however, the hyperfine parameters of the doublet were considerably different (for Fe-Si, IS$=0.45$ mm/sec, QS$=0.99$ mm/sec; and for Fe-Ge, IS$=0.40$ mm/sec, QS$=0.88$ mm/sec, where IS and QS represent isomer-shift and quadrupole-splitting parameters, respectively), as compared to the present case of Fe-Al interface. Hence, the central doublet is undoubtedly caused by a deposition-induced reaction between iron and the aluminum surface. The third possibility, viz., formation of a phase of Fe-Al system having dilute concentration of iron which comes under this category could be eliminated rather easily because our spectrum corresponding to the as-deposited sample could not be fitted with the known hyperfine parameters of $FeAl_6$ or those of any other dilute-Fe phases of the Fe-Al system, such as, Fe_4Al_{13}, etc. The CEMS spectrum could not be fitted even though the fitting was attempted with values of hyperfine parameters close to those for the dilute-Fe phases. These facts along with the other points mentioned above clearly indicate that the central doublet can be attributed to the incorporation of a small quantity of ^{57}Fe of the interface layer into the thin γ-Al_2O_3 skin which is always present on the aluminum surface.

The x-ray diffraction results corresponding to the as-deposited sample show a significant contribution of the [110] and [200] planes of Fe and a small contribution of the dominant [111] planes corresponding to aluminum. This is indeed to be expected on the basis of the fact that in the small-angle x-ray scattering mode the x-rays traverse a long path length in the iron overlayer and a relatively smaller path length below the interface region. This x-ray data, although not very useful in ascertaining the atomistic aspects of the physical state of the interface, can certainly serve as a confirmatory support for the conclusion derived on the basis of CEMS measurements, especially in the case of the ion-beam-mixed sample with and without thermal annealing treatment, as will be seen later.

The CEMS spectrum of the ion-beam-mixed sample is shown in Fig. 2(b). This spectrum is substantially different from that of the as-deposited sample. Besides the central component, the spectrum clearly shows the existence of a distribution of hf field. When decomposed using the standard procedure mentioned earlier, this spectrum gives the $P(H)$ distribution as shown in Fig. 2(f). This distribution exhibits four distinct peaks at 100, 192, 252, and 330 kOe. On comparing the P(H) distribution for the as-deposited sample [Fig. 2(e)] and that for the ion-beam-mixed sample [Fig. 2(f)], one finds that the peak at ~ 330 kOe (characteristic of α-Fe) is considerably reduced in the mixed sample with a very slight change in the peak at ~ 252 kOe and emergence of two additional peaks at 192 and 100 kOe. CEMS spectrum not only shows that atomic mixing has taken place but also the varying environment experienced by ^{57}Fe atoms in the mixed zone.

In order to understand the observed distribution of hf field indicative of the varying nature of the environment of ^{57}Fe atoms in the mixed zone, it is necessary to briefly discuss the mechanism of ion-beam-induced atomic mixing. When 100-keV Ar^+ ions are incident on a composite of Al substrate overcoated with iron film, they penetrate into the composite to an average depth of ~ 300 Å. In the process, they cause a series of branching cascades of atomic collisions pushing iron atoms across the interface into aluminum substrate with an outmigration of aluminum; and create a number of vacancies and interstitials. The whole process occurs extremely rapidly over a time scale of 10^{-13} to 10^{-10} sec leading to the quenching of the mixed zone into a metastable alloy. It has been shown that when the structures of the two components, such as Fe (bcc) and Al (fcc) in the present case, are different a random alloy is formed on ion-beam-induced mixing.[11] However, there is no information available in the litera-

ture about the atomic coordination in the mixed zone. In the present case, the coordination in Fe (bcc) being 8 (nearest neighbors) and in Al (fcc) being 12, it is possible that in the mixed zone (i.e., in the random alloy) the coordination varies randomly between 8 and 12. Above the mixed zone, one may expect to have iron with a few Al atoms, whereas below the mixed zone a dilute concentration of iron in aluminum is expected.

Assuming the average composition of the mixed zone to be $Fe_{55}Al_{45}$, one can obtain the probability $P(n)$ of a given Fe atom having n nearest Al neighbors in 8 and 12 coordination configurations by using the standard binomial distribution given by

$$P(n)=\frac{N!}{n!(N-n)!}C^n(1-C)^{(N-n)},$$

where N is the atomic coordination (8 or 12) and C is the Al concentration in the random alloy. If we further assume that the hf field at ^{57}Fe nucleus decreases progressively at a rate of $\sim$26 kOe per nonmagnetic aluminum neighbor[27–29] one can transform the distribution function $P(n)$ to give the distribution of the hf field $P(H)$ as shown in Fig. 3. This $P(H)$ distribution curve shows peaks at 190 and 252 kOe. It is interesting to note that peaks at these values of hf field are indeed observed in the case of the ion-beam-mixed sample [Fig. 2(f)] and by comparing the relative intensities of the two peaks it is possible to find the proportion of iron atoms with coordination 8 and 12.

It may be noticed [Fig. 2(f)] that in addition to the two peaks at 190 and 252 kOe, the ion-beam-mixed sample also shows one peak at 330 kOe and the other at 100 kOe. The CEMS spectrum of this sample [Fig. 2(b)] also has a contribution of a doublet with an isomer shift of 0.3 mm/sec and a quadrupole splitting of 0.947 mm/sec. The peak at 330 kOe is undoubtedly the peak due to α-Fe contributed by ^{57}Fe atoms above the mixed zone. The observation of a peak at 100 kOe in the $P(H)$ curve and a doublet near zero velocity position indicate that the ^{57}Fe atoms responsible for these signals are in weakly magnetic

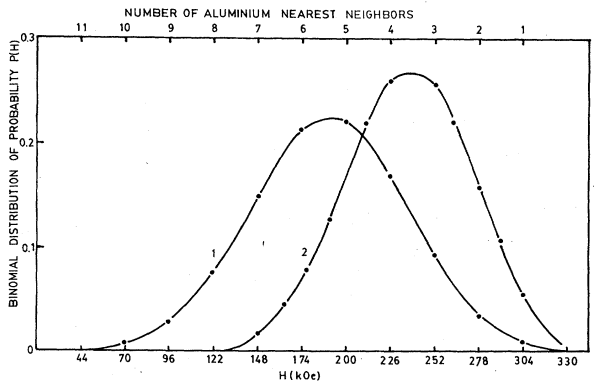

FIG. 3. Probability distribution function $P(n)$ for n Al atoms to be near neighbors to an Fe atom in a random alloy $Fe_{55}Al_{45}$ using the standard binomial distribution; the corresponding hyperfine field distribution $P(H)$ for local atomic coordination 12 (curve 1) and 8 (curve 2).

and nonmagnetic environments, respectively. Such an environment is expected in the layers below the mixed zone where one has dilute Fe concentration in Al matrix. This situation can be favorably compared to the case of low dose implantation of ^{57}Fe in aluminum. Such experiments have been carried out by Sawicka *et al.*[30] They have reported that up to 5 at. % concentration of ^{57}Fe in Al, the Mössbauer spectrum is composed of a single line and a quadrupole-split doublet. The contribution of the single line decreases as the concentration of Fe increases and above 5 at. % of Fe, only a doublet is seen. These authors attributed the doublet to Fe dimers in Al. They have also reported that the isomer shift and the quadrupole splitting of the doublet increases with a further increase of Fe concentration. It is therefore reasonable to assume that the central quadrupole doublet observed in the spectrum [Fig. 2(b)] of the ion-beam-mixed sample is essentially due to Fe dimers in Al. If the aggregation of Fe in Al increases further to form, say, trimers or higher associations, the configuration could become weakly magnetic with hf field of 100 kOe.

The x-ray diffraction result corresponding to the ion-beam-mixed sample in the as-mixed state [Fig. 5(b)] clearly shows a significant rise in the background level of the diffraction pattern indicating the presence of disorder. In addition to an enhancement of the extent of contribution in the region of 2θ just below the main diffraction peak corresponding to α-Fe [110], one can observe a broad hump in the pattern in the region of 2θ between 26° and 34°. Both these features can be attributed to the occurrence of an atomic mixing at the interface, because the significant diffraction peaks corresponding to a large number of phases of the Fe-Al system fall at 2θ values which are somewhat lower than 45.06° which corresponds to the dominant [110] diffraction peak of α-Fe, while other dominant diffraction peaks fall in the range between 2θ values of 26° and 32°. The fact that the x-ray-diffraction pattern does not show a well-define peak structure (not referring to the sharp lines due to α-Fe in the top unmixed portion of the sample) is consistent with the CEMS observation of broad distribution of internal magnetic field [Fig. 2(f)] indicative of variations in the atomic environment experienced by the ^{57}Fe nuclei.

The CEMS spectra of the ion-beam-mixed sample annealed at 300 °C and 400 °C for 20 min each, do not show any significant changes. These spectra [Figs. 2(c) and 2(d)] were decomposed to give the hf field distribution [Figs. 2(g) and 2(h)]. It is seen that the hf field distribution in these cases is identical to what was observed for the unannealed ion-beam-mixed sample. These results clearly indicate that no significant atomic motion is possible at these temperatures and that the mixed zone continues to be in a metastable random-alloy phase with an average composition of $Fe_{55}Al_{45}$.

On annealing, the ion-beam-mixed sample at 500 °C for 20 min, a sudden phase precipitation appears to have occurred resulting in a sharp hf split pattern [Fig. 4(a)]. The x-ray-diffraction result corresponding to this sample [Fig. 5(c)] is also vastly different from that of the ion-beam-mixed sample in the as-mixed state [Fig. 5(b)]. The CEMS spectrum of Fig. 4(a) can be fitted with two sextets

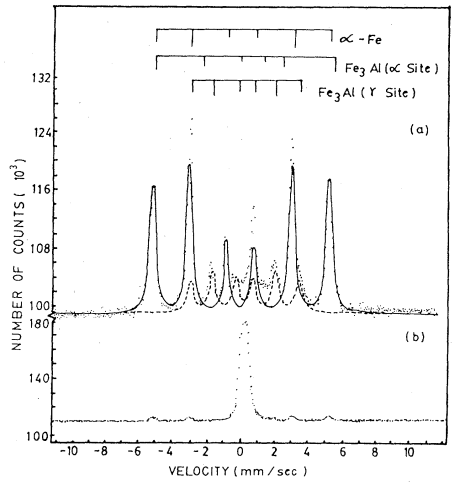

FIG. 4. Room-temperature conversion-electron Mössbauer spectra of ion-beam-mixed samples annealed (a) at 500 °C showing the precipitation of Fe and Fe_3Al phases and (b) at 600 °C showing the formation of iron clusters.

corresponding to hf fields of 328 and 210 kOe. The former is undoubtedly due to the α-Fe phase. The other sextet with a hf field of 210 kOe has an isomer shift of 0.17 mm/sec and is typically characteristic of Fe_3Al. Stochiometric Fe_3Al has an ordered DO_3-type lattice with a unit cell having α, β, and γ sites.[18] The α and γ sites are occupied by Fe atoms whereas the β sites are occupied by Al atoms. ^{57}Fe Mössbauer spectrum of ordered Fe_3Al as reported by Czjzek and Berger[31] shows two superposed six-finger patterns with an internal field of 210 kOe (Fe at γ sites with four nearest Fe neighbors) and 295 kOe (Fe at α sites with eight nearest Fe neighbors). Although at the α site, the Fe atoms have the same number of near neighbors as in α-Fe, the hf field at ^{57}Fe nucleus at the α site is less than that observed at ^{57}Fe nucleus in α-Fe. This difference has been attributed to the presence of Al atoms in the neighborhood. If there are vacancies at normal Al sites, then the field at ^{57}Fe nucleus in α sites would be almost equal to that at ^{57}Fe in α-Fe, i.e., 330 kOe. It is also necessary to mention that the sextet with a hf field of 210 kOe is twice as strong as the sextet with a hf field of 295 kOe in ordered Fe_3Al. In our case, as mentioned above, we observed only a sextet with a hf field of 210 kOe and did not observe the other weaker sextet with a hyperfine field of 295 kOe. This nonobservance of the other sextet may be due to the fact that the Fe_3Al which is formed on annealing of the ion-beam-mixed sample at 500 °C is not completely ordered; or the Fe atoms in α sites have Al vacancies in their neighborhood, thereby increasing the hf beyond 295 kOe and leading to overlap of this contribution with sextet due to α-Fe.

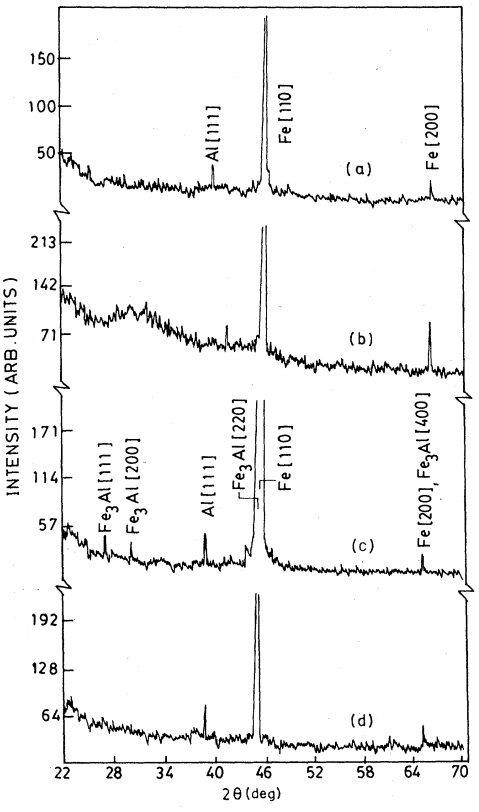

FIG. 5. X-ray-diffraction patterns of (a) as-deposited and [(b)—(d)] ion-beam-mixed Fe-Al composites. The x-ray-diffraction patterns of (c) and (d) correspond to the ion-beam-mixed composite annealed at 500 °C and 600 °C, respectively, for 20 min each.

The inferences in the above paragraph concerning the physical state of the ion-beam-mixed sample annealed at 500 °C made on the basis of CEMS measurements are once again found to be in complete agreement with the x-ray-diffraction results [Fig. 5(c)]. The x-ray results clearly bring out the contributions of the dominant [220], [111], [200], and [400] planes corresponding to the Fe_3Al phase, which appear at 2θ values of 44.36°, 26.66°, 30.92°, and 64.18°, respectively. In fact, the presence of the strongest Fe_3Al diffraction peak at 2θ value of 44.36° which is just below the strongest α-Fe diffraction peak at 2θ value of 45.06° is clearly reflected in the appearance of a broad line in this region of diffraction. It is also significant to note that the background absorption level which was considerably high in the as-mixed sample is also substantially reduced upon annealing; indicating elimination of structural disorder and phase precipitation.

The sudden and marked change in the Mössbauer spectrum on annealing the ion-beam-mixed sample at 500 °C suggests that at this temperature, significant atomic motion becomes possible enabling the transformation of metastable random alloy $Fe_{55}Al_{45}$ into stable Fe_3Al and α-Fe. Assuming that this phase precipitation is due to atomic migration over a few lattice units during the annealing time, one can estimate the atomic diffusion coefficient of Fe-Al in the mixed phase. This atomic diffusion coefficient turns out to be of the order of 10^{-21} cm^2/sec. It is very interesting that Hirvonen and Räisanen[32] have reported that the diffusion coefficient of Al in ion-implanted Fe is 3.1×10^{-21} cm^2/sec at 500 °C. This value agrees remarkably well with the value of the diffusion coefficient inferred by us.

On further annealing the samples at 600 °C for 20 min, one observes the CEMS spectrum as shown in Fig. 4(b).

This spectrum is significantly different from the one corresponding to the sample annealed at 500 °C. The CEMS spectrum of the sample annealed at 600 °C can be fitted to a sextet with a hf field of 330 kOe characteristic of α-Fe and a quadrupole-split doublet with an isomer shift of 0.17 mm/sec and a quadrupole splitting of 0.30 mm/sec. In order to uniquely ascertain the physical state of the interface responsible for the occurrence of the quadrupole doublet one may use the x-ray-diffraction result for the sample annealed at 600 °C [Fig. 5(d)]. This x-ray pattern shows the presence of only α-Fe and Al in the sample; and complete absence of the lines corresponding to the Fe_3Al phase, which were present in the sample annealed at 500 °C. It may in fact be noted that in Fig. 5(d) a sharp line is observed at a 2θ value of 45.06° corresponding to α-Fe and the line at 44.36° corresponding to Fe_3Al [220] is completely eliminated. The other lines corresponding to Fe_3Al at 2θ values of 26.66°, 30.92°, and 64.18° are also absent in the x-ray diffraction result of Fig. 5(d). It may thus be concluded that the intermediate metastable Fe_3Al phase formed in the ion-beam-mixed sample annealed at 500 °C is decomposed upon annealing at 600 °C leading to a phase-separated system of iron and aluminum. If the entire iron in the phase separated state were bulklike, then only a six-finger pattern would have been observed in the CEMS spectrum. The presence of a major contribution of a quadrupole-split doublet in the spectrum, however, clearly shows that a substantial fraction of iron at the interface is in the form of iron clusters in aluminum matrix. It is indeed gratifying to note that the hyperfine interaction parameters of the quadrupole-split doublet in the CEMS spectrum of Fig. 4(b) match extremely well with those of iron clusters in aluminum, reported by Nasu *et al.*[33] Thus, in conclusion it may be stated that annealing of the ion-beam-mixed sample at 600° leads to disintegration of the intermediate metastable phase formed at the interface due to annealing at 500 °C, to form iron clusters in aluminum matrix.

Finally, it is of interest to point out the characteristic difference between ion-beam processing and thermal processing of the Fe-Al composite. When the as-deposited Fe-Al composite is annealed at 300 °C and 400 °C, one finds hardly any change in the Mössbauer spectrum from the spectrum corresponding to the as-deposited sample. However, on annealing the as-deposited sample at 500 °C one observes only a spectrum characteristic of α-Fe. This shows out-migration of Fe. In contrast, in case of ion-beam-mixed sample annealed at 500 °C one observes a change from a random alloy with an average composition of $Fe_{55}Al_{45}$ to give α-Fe and Fe_3Al. Similarly, the as-deposited sample thermally annealed at 600 °C shows only a spectrum characteristic of α-Fe without any doublet as is observed in the ion-beam-mixed sample annealed at 600°.

B. Dose dependence of ion-beam mixing (non-interface-sensitive CEMS measurements)

A study of the dependence of ion-beam-induced mixing on the implantation dose is of considerable importance from two points of view. Firstly, it is of interest to identify the range of ion dose which could yield efficient atomic mixing in the case of a given binary system and to establish the correlation between such dose range and the physical properties of the participating elements. Secondly, from the standpoint of physics it is of importance to know the change in the nature of the beam-mixing process as the ion dose is increased from the low dose regime corresponding to isolated cascade effects to the high dose regime which involves cascade overlap effects. Some experimental work on the growth of the beam-mixed region at the interface as a function of the ion dose has been reported in the literature;[34] however, no detailed information regarding the microscopic aspects of the dose dependence of ion-beam mixing is presently available. Since Mössbauer spectroscopy can bring out such an information at an atomic level we undertook the study of the dose dependence of ion-beam mixing by employing the CEMS technique. In this case we resorted to the non-interface-sensitive studies for the reason which has been clearly mentioned earlier.

The CEMS spectrum of the as-deposited sample and the corresponding field distribution [$P(H)$] appear as shown in Figs. 6(a) and 6(h), respectively. Since the ^{57}Fe

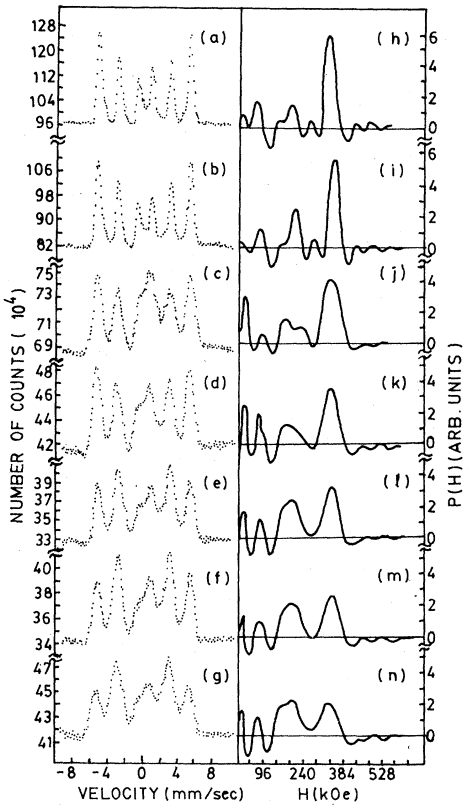

FIG. 6. Room-temperature conversion-electron Mössbauer spectra of (a) as-deposited and (b)—(g) ion-beam-mixed Fe-Al composites. The implantation dose values of 100-keV Ar^+ ions corresponding to the CEMS spectra of (b), (c), (d), (e), (f), and (g) are 1×10^{14}, 5×10^{14}, 1×10^{15} 5×10^{15}, 1×10^{16}, and 3×10^{16} ions/cm^2, respectively. The $P(H)$ distribution curves corresponding to the CEMS spectra of (a), (b), (c), (d), (e), (f), and (g) are given in (h), (i), (j), (k), (l), (m), and (n), respectively.

nuclei are uniformly distributed in the overlayer, most of them experience an α-Fe-like environment with a single hyperfine field of 330 kOe. The ratios of line intensities are 3:2:1::1:2:3 and these represent the random magnetization direction in iron film.[15] The CEMS spectra of Fe-Al composites bombarded with 100-keV Ar^+ ions at doses between 10^{14} and 3×10^{16} ions/cm^2 are shown in Figs 6(b)—6(g) and corresponding $P(H)$ distributions are given in Figs. 6(i)—6(n), respectively. The systematic change in the nature of the CEMS spectrum as well as the $P(H)$ distribution can be clearly observed in these results. The gradual decrease of the peak at 330 kOe in the $P(H)$ curve and the increase of low field components clearly signify that increase in ion dose leads to atomic mixing of increasing number of Fe atoms with the nonmagnetic Al atoms.[27] It may be noticed that the spectral component near zero velocity channel shows a small increase in intensity upon bombardment at 10^{14} ions/cm^2 and a sudden increase subsequent to bombardment at 5×10^{14} ions/cm^2. The linewidths are also considerably larger in the latter case and these features of disorder are directly reflected in the $P(H)$ curve [Fig. 6(j)]. As the dose is increase beyond 5×10^{14} ions/cm^2, however, the changes appear to be more gradual; the main features of the changes being variations of line intensity ratios and linewidths. The peak at 330 kOe (due to α-Fe of the unmixed portion of the overlayer) also shows a decrease accompanied by broadening of the peakwidth. The low field components exhibit a gradual increase in intensity without any drastic change in the nature of their distribution. It is of interest to study the dependence of the total contribution of the low field components on ion dose because these components reflect the extent of atomic mixing of the magnetic Fe atoms with the nonmagnetic Al atoms. This dependence is shown in Fig. 7. It may be clearly seen that the rate of growth of the mixed region shows a significant decrease when the dose rises above 5×10^{14} ions/cm^2. Considering the fact that at dose values above 5×10^{14} ions/cm^2 the cascade overlap effects[35] start dominating the mixing process, the change in the nature of the mixing reaction at this dose value can be attributed to ensuance of such effects. It may be argued[35] that at doses below 5×10^{14} ions/cm^2 the mixing occurs mainly via individual cascade effects which cause vacancy generation across the interface leading to a rapid growth of the mixed region. At these doses the contribution of cascade overlap effect may be expected to be rather small (although not negligible). On the other hand, if bombardment is continued beyond the dose of 5×10^{14} ions/cm^2 the energy deposited by ions may be dispersed in the medium by defect-assisted long-range atomic transport in the film. Such transport can primarily occur within the premixed region wherein a large concentration of defects already persists, leading to a slower increase in the mixed region across the interface.

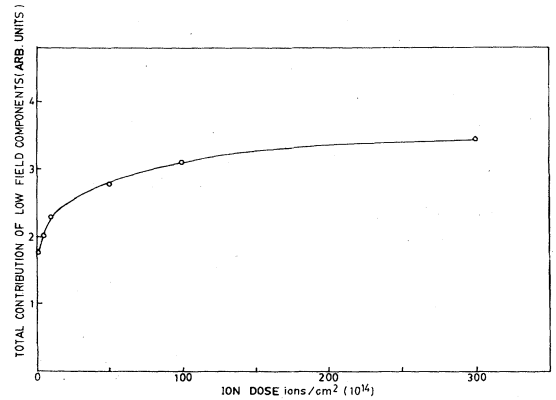

FIG. 7. Dependence of low internal magnetic field components (corresponding to ^{57}Fe atoms with one or more aluminum neighbors) on the implantation dose.

It has been suggested[35] that an increase of ion dose above $\sim10^{15}$ ions/cm^2 primarily leads to dilution of the mixed region and densification of the regions above and below the central mixed zone. This can lead to generation of stress in the mixed region and to a magnetic anisotropy via magnetostrictive coupling, provided the film has a ferromagnetic nature. This is clearly established by our results which show a systematic change in the line intensity ratios[15] from 3:2:1::1:2:3 in the as-deposited sample exhibiting random direction of magnetization, to 3:4:1::1:4:3 in the sample bombarded with ion dose of 3×10^{16} ions/cm^2 indicating presence of magnetization in the plane of the film in the beam-mixed alloy. At doses between 5×10^{14} and 3×10^{16} ions/cm^2 the intensity ratios show a systematic variation indicating gradual build up of stress.

In addition to the Fourier decomposition procedure we also used a conventional Mössbauer fitting method to obtain hf interaction parameters. In samples bombarded at 10^{14}, 5×10^{14}, 10^{15}, and 5×10^{15} ions/cm^2 we could clearly identify the contributions of Fe monomers and dimers in Al[10] in addition to the magnetic components. The monomer contribution decreases from $\sim11\%$ to $\sim0.5\%$ when the dose is increased from 10^{14} to 5×10^{15} ions/cm^2. On the other hand, the contribution of dimers shows a gradual increase with ion dose over the entire dose range between 10^{14} ions/cm^2 to 3×10^{16} ions/cm^2, increasing from $\sim4\%$ to $\sim12\%$. The decrease of monomer contribution and the simultaneous increase of dimer contribution indicates the tendency of Fe atoms to form associations in Al matrix under chemically and structurally metastable conditions. The isomer shift, quadrupole splitting, and the linewidth corresponding to the quadrupole-split doublet representing the dimers also show gradual increase from their values of 0.25, 0.90, and 0.34 mm/sec, respectively, for samples mixed at a dose of 10^{14} ions/cm^2, to 0.61, 1.07, and 0.46 mm/sec, respectively, for a sample mixed at a dose of 3×10^{16} ions/cm^2. Such an increase in the values of hf interaction parameters (especially the isomer shift) with ion dose once again supports the view that mixing by using progressively higher dose leads to dilution of the mixed region.[35] This is because such a dilution can cause a decrease in the value of S-electron density at iron nucleus and correspondingly an increase of isomer shift.[15]

IV. CONCLUSION

The physical processes associated with ion-beam-induced reactions at the Fe-Al interface have been studied

for the first time using the method of conversion-electron Mössbauer spectroscopy, which has been made interface sensitive by enriching the interface layers with ^{57}Fe Mössbauer isotope. A non-interface-sensitive study has also been performed to investigate the dose dependence of ion-beam mixing.

Ion-beam mixing of Fe-Al composite (100-keV Ar^+ ions, ion dose $\sim 10^{16}$ ions/cm^2) produces a metastable random alloy with a composition $Fe_{55}Al_{45}$. The Fe atoms in this alloy experience varying atomic environment which is reflected by the distribution of the hyperfine field at ^{57}Fe nuclei. Atomic migration in this metastable alloy is initiated at 500 °C and it leads to the formation of Fe_3Al and α-Fe phases. Further annealing of the ion-beam-mixed sample at 600 °C disintegrates the Fe_3Al phase to give iron clusters in Al matrix. In so far as the dose dependence of ion-beam mixing is concerned a significant change in the mixing reactions is seen to occur when the ion dose increases above $\sim 10^{15}$ ions/cm^2, which corresponds to a dose value beyond which the cascade overlap effects start becoming increasingly important.

ACKNOWLEDGMENTS

Two of us (V.P.G. and S.M.C.) gratefully acknowledge the financial assistance by the Department of Atomic Energy and the Defence Research and Development Board (Government of India), respectively. The authors are grateful to Professor G. K. Mehta and Dr. Naik of Indian Institute of Technology (Kanpur), India for allowing the use of their facilities for RBS work. Thanks are also due to Dr. L. Lowry of Materials Laboratory (JPL), California Institute of Technology for carrying out small-angle x-ray-diffraction measurements on our samples. This work was supported by the Department of Science and Technology, Government of India.

[1]J. W. Mayer, L. Erikson, and J. A. Davies, *Ion Implantation in Semiconductors* (Academic, New York, 1970).

[2]*Ion Implantation in Semiconductors and other Materials,* edited by B. L. Crowder (Plenum, New York, 1973).

[3]B. Y. Tsaur, Z. L. Liau, and J. W. Mayer, Appl. Phys. Lett. **34**, 168 (1979).

[4]B. Y. Tsaur, Z. L. Liau, and J. W. Mayer, Phys. Lett. **71A**, 270 (1979).

[5]B. Y. Tsaur, S. S. Lau, and J. W. Mayer, Appl. Phys. Lett. **35**, 225 (1979).

[6]B. Y. Tsaur, J. W. Mayer, and K. N. Tu, J. Appl. Phys. **51**, 5326 (1980).

[7]B. Y. Tsaur, J. W. Mayer, J. F. Graczyk and K. N. Tu, J. Appl. Phys. **51**, 5334 (1980).

[8]J. W. Mayer, B. Y. Tsaur, S. S. Lau, and L. S. Hung, Nucl. Instrum. Methods **182-183**, 1 (1981).

[9]B. Y. Tsaur, S. S. Lau, L. S. Hung, and J. W. Mayer, Nucl. Instrum. Methods **182-183**, 67 (1981).

[10]S. S. Lau, B. Y. Tsaur, M. Allmen, J. W. Mayer, B. Stritzker, C. W. White, and B. Appleton, Nucl. Instrum. Methods **182-183**, 97 (1981).

[11]B. X. Liu, W. L. Johnson, M. A. Nicolet, and S. S. Lau, Appl. Phys. Lett. **42**, 45 (1983).

[12]V. P. Godbole, V. G. Bhide, S. V. Ghaisas, A. Murthy, S. K. Kulkarni, and S. B. Ogale, Nucl. Instrum. Methods **209-210** 131 (1983).

[13]D. K. Sood (private communication).

[14]B. M. Paine, M. A. Nicolet, R. G. NewCombe, and D. A. Thompson, Nucl. Instrum. and Methods **182-183**, 115 (1981).

[15]V. G. Bhide, *Mössbauer Effect and Its Applications* (Tata McGraw-Hill, New Delhi, 1973).

[16]B. D. Sawicka and J. A. Sawicki, in *Topics in Current Physics: Mossbauer Spectroscopy-II,* edited by U. Gonser (Springer, Berlin, 1981).

[17]R. Feder and B. S. Berry, J. Appl. Crystallogr. **3**, 372 (1970).

[18]U. Gonser and Moshe Ron, in *Applications of Mossbauer Spectroscopy,* edited by R. L. Cohen (Academic, New York, 1980), Vol. II.

[19]S. B. Ogale, S. V. Ghaisas, A. S. Ogale, V. N. Bhoraskar, A. S. Nigavekar, and M. R. Bhiday, Radiat. Eff. **63**, 73 (1982).

[20]This MOSFIT program was originally written by E. Kreber from Universite des Saarlandes, Saarbruken and it was adopted for ICL 1904S computer by S. K. Date from National Chemical Laboratory, Pune, India.

[21]B. Window, J. Phys. E **4**, 401 (1971).

[22]R. S. Preston, Metall. Trans. **3**, 1831 (1972).

[23]M. B. Stearns, Phys. Rev. **147**, 439 (1966).

[24]W. Kundig, H. Bommel, G. Canstabaris, and R. H. Lindquist, Phys. Rev. **142**, 327 (1966).

[25]S. B. Ogale, Rekha Joshee, V. P. Godbole, S. M. Kanetkar, and V. G. Bhide, J. Appl. Phys. (to be published).

[26]Jayashree Patankar, Y. V. Bhandarkar, S. M. Kanetkar, S. B. Ogale, and V. G. Bhide, Nucl. Instrum. Methods (to be published).

[27]M. B. Stearns, Phys. Rev. **129**, 1136 (1963).

[28]G. Marchal, Ph. Mangin, and Chr. Janot, Solid State Commun. **18**, 739 (1976).

[29]L. Häggström, L. Gränäs, R. Wäppling, and S. Devanarayanan, Phys. Scr. **7**, 125 (1973).

[30]B. D. Sawicka, M. Drwiega, J. A. Sawicki, and J. Stanek, Hyperfine Interact. **5**, 147 (1978).

[31]G. Czjzek and W. G. Berger, Phys. Rev. B **1**, 957 (1970).

[32]J. Hirvonen and J. Räisanen, J. Appl. Phys. **53**, 3314 (1982).

[33]S. Nasu, U. Gonser, and R. S. Preston, J. Phys. (Paris) Colloq. **41**, C1-385 (1980).

[34]J. W. Mayer and S. S. Lau, in *Surface Modification and Alloying by Laser, Ion and Electron Beams,* edited by J. M. Poate, G. Foti, and D. C. Jacobson (Plenum, New York, 1981).

[35]J. A. Davies, in *Surface Modification and Alloying by Laser, Ion and Electron Beams,* edited by J. M. Poate, G. Foti, and D. C. Jacobson (Plenum, New York, London, 1981).